Supporting Information

Weber et al. 10.1073/pnas.1003052107

SI Text

Identifying Candidate Host Materials. It is straightforward to identify tetrahedrally coordinated semiconductors that satisfy criteria H1–H4 outlined in the main text. First, band-structure parameters can be used to identify hosts that satisfy H1 and H2. In Table S1, we list a number of tetrahedrally coordinated hosts whose band gaps are larger 2.0 eV (diamond, Si, and GaAs are listed in the bottom three rows for comparison). Whereas 2.0 eV is an arbitrarily defined value, we would like to accommodate deep centers whose optical transitions lie in the near-infrared (0.89–1.65 eV) or visible (1.65–3.10 eV) regions of the electromagnetic spectrum because optical equipment compatible with these energies is widely available. The band-gap energy (E_g) of each host is listed in the second column. In the third column, we list the spin-orbit splitting (Δ_{SO}) of each material, as taken from valence-band splitting(s) at the Γ point. Although Δ_{SO} is not a direct measure of the spin-orbit coupling in a host, it is still indicative of the strength of the spin-orbit interaction. Values of E_g and Δ_{SO} are room-temperature values unless otherwise noted. In materials where more than one crystal structure is stable at room temperature, we have chosen to display the band parameters for the dominant room-temperature phase.

In the fourth column of the table, we list whether stable isotopes with nuclear spin equal to zero exist for the atomic species of each compound (criterion H4). We note that, whereas the lack of a nuclear spin bath may help to increase the spin-coherence time of a paramagnetic deep center, H4 is not necessarily a strict requirement. It is beyond the scope of this paper to address the question of whether current growth technologies for each material are compatible with isotopic engineering, but it should be noted that the natural abundance of spin-0 isotopes varies by atomic species.

All of the hosts listed can be grown as single crystals, but the quality currently varies widely by material. For instance, the types and numbers of extended defects that one may expect in a state-of-the-art growth of each host varies widely by material, as does the current maximum single-crystal size. Nevertheless, many of the materials listed (such as 4H-SiC, ZnO, and GaN) can be bought commercially as wafers an inch or more in diameter.

Trends in Defect-Level Splitting. Although detailed calculations are necessary to systematically determine the splitting and location of defect levels, important insights are provided by the behavior of interacting dangling-bond (DB) orbitals that give rise to the defect levels, as shown in Fig. 5 of the main text. These DB orbitals are closely related to the sp^3 orbitals in a tetrahedrally coordinated semiconductor. To demonstrate these concepts with a specific example, let us consider a cation vacancy (CV) in a tetrahedral semiconductor (surrounded by interacting anion DBs as depicted in the lower half of Fig. 5). As discussed in the main text, the t_2 vacancy levels tend to be located in the lower half of the band gap. Here we address how the choice of host and defect center impacts the energy position of the anion DB orbitals, and the splitting between the a_1 and t_2 vacancy orbitals (Δ_{CV}, Fig. 5*B*).

As the anion becomes more electronegative, i.e., closer to the upper right corner of the periodic table, the energy of its atomic *s* and *p* orbitals decreases and the orbitals become more localized. The overlap of these sp^3 DB orbitals determines the splitting Δ_{CV} between the vacancy levels as illustrated in Fig. 5*B*. This overlap is determined by the degree of localization of the sp^3 orbitals and by the spatial separation between the anions, which in turn is related to the lattice constant of the material; a larger lattice constant leads to larger anion-anion separation and hence a decrease in Δ_{CV}. We note that for a given anion, lattice parameters increase with atomic number of the cation. Thus, as we move down the periodic table, the lattice constant will increase and Δ_{CV} will decrease. One can exploit these trends to engineer defects with vacancy levels in the desired energy range. The trends are less clear when fixing the choice of cation and selecting different anions, because moving down the periodic table increases the lattice constant but decreases the localization of the sp^3 orbitals, resulting in less predictable effects on the Δ_{CV} splitting. Anion vacancies are even more complicated, as discussed in the main text.

Electron Counting for Defects. As discussed in the main text, the occupation of defect levels determines the defect's spin state and whether a spin-conserving triplet excitation can occur. Electron counting is a useful tool to determine which charge state will produce the proper spin for such an excitation. Considering a tetrahedrally coordinated compound semiconductor AB, we envision creating a vacancy on the B site (V_B), surrounded by sp^3 DBs on the neighboring A atoms that give rise to a_1 and t_2 vacancy levels (Fig. S1 *A* and *B*). If a substitutional impurity (X) is placed onto an A site that neighbors the vacancy (Fig. S1*C*), the defect levels will further split into $a_1(1)$, $a_1(2)$, e_x, and e_y as a consequence of the reduced symmetry.

These resulting defect levels can be filled with electrons in various ways, depending on the charge state. For defects analogous to the NV^{-1} defect in diamond, the $a_1(1)$ level will be well below the VBM, as shown schematically in Fig. 2. Assuming this is the case, we can fill the remaining gap levels to obtain the desired spin-one configurations. Fig. S2 outlines the two possibilities. Six electrons are needed to create a configuration similar to the NV^{-1} in diamond, which has two electrons in the $a_1(2)$ level, and one electron in each of the e_i levels (Fig. 2*A*). This configuration allows for a spin-conserving transition between the spin-minority $a_1(2)$ and e_i levels. In addition, a four-electron configuration also exists with a spin-triplet ground state (Fig. S2*B*), as was discussed for the V_{Si}^0 defect in SiC. This configuration allows for a spin-conserving transition between the spin-majority $a_1(2)$ and e_y levels, as shown in Fig. 3*D* of the main text.

Now that we understand how many electrons are needed to form ground-state triplets in these configurations, we can determine which defect charge states are needed to produce such occupations. The charge state Q of the defect is given by

$$Q = 4 \times \frac{N_A}{4} + (N_X - N_A) - n_e = N_X - n_e, \qquad \text{[S1]}$$

where n_e is the total number of electrons in the defect levels, and N_A (N_X) the number of valence electrons for atom A (X). For example, $n_e = 6$ for the $N_C V_{Si}$ center in SiC, as discussed in the main text. Furthermore, $N_X = 5$ because atom X is a nitrogen atom. Hence, $Q = -1$, as noted in the main text.

As another example, consider the Zn vacancy (V_{Zn}) in ZnSe, which has been calculated to be stable in the 0, −1, and −2 charge states (1). In the neutral charge state ($Q = 0$) of V_{Zn}, and with $N_X = N_A = 6$ (because there is no impurity present), Eq. **S1** shows that $n_e = 6$, and thus a spin-triplet ground state similar to Fig. S2*A* is stable. In addition, we can place an impurity next to the vacancy. If we focus on group-VII atoms, which act as donors on the oxygen site and are electrostatically attracted to the vacancy, $N_X = 7$ and $n_e = 6$, so that $Q = +1$.

In this discussion we have considered only the number of electrons needed to fill defect levels similar to those shown in Fig. S2. To properly address broader issues, such as whether defect levels are sufficiently deep in the band gap and whether criteria D1–D5 can be satisfied, explicit first-principles calculations are needed for each defect in question.

1. Laks DB, Van de Walle CG, Neumark GF, Blöchl PE, Pantelides ST (1992) Native defects and self-compensation in ZnSe. *Phys Rev B* 45:10965.

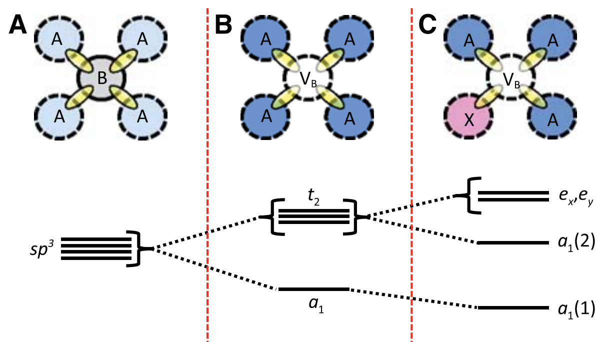

Fig. S1. Development of defect-level structure in tetrahedrally coordinated (AB) compound semiconductors. Atomic sp^3 dangling bonds (*A*) interact to form a_1 and t_2 levels in an ideal vacancy (*B*), with the t_2 levels splitting further in vacancy complexes (*C*).

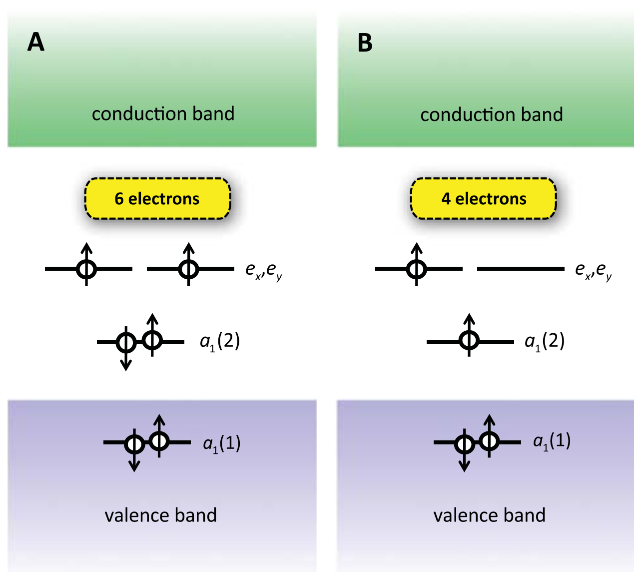

Fig. S2. Schematic defect-level diagrams for vacancy-related complexes in tetrahedrally coordinated semiconductors. These diagrams show defect levels with an occupation of six (*A*) and four (*B*) electrons.

Table S1. Host material parameters

Material	Band gap, E_g (eV)	Spin-orbit splitting, Δ_{SO} (meV)	Stable spinless nuclear isotopes?
3C-SiC	2.39 (2 K)	10 (2 K)	Yes
4H-SiC	3.26 (4 K)	6.8 (2 K)*	Yes
6H-SiC	3.02 (4 K)	7.1 (2 K)	Yes
AlN	6.13	19 (theory)†	No
GaN	3.44	17.0 (10 K)	No
AlP	2.45	50 (theory)‡	No
GaP	2.27	80	No
AlAs	2.15	275	No
ZnO	3.44 (6 K)	−3.5 (6 K)	Yes
ZnS	3.72	64	Yes
ZnSe	2.82 (6 K)	420	Yes
ZnTe	2.25	970 (80 K)	Yes
CdS	2.48	67 (10 K)	Yes
Diamond (C)	5.5	6 (1.2 K)	Yes
Si	1.12	44 (1.8 K)	Yes
GaAs	1.42	346 (1.7 K)	No

All values of E_g and Δ_{SO} are room-temperature values and are taken from ref. 1 below, unless noted otherwise.
*Data taken from ref. 2 below.
†Data taken from ref. 3 below.
‡Data taken from ref. 4 below.

1 Madelung O (2004) *Semiconductors: Data Handbook* (Springer–Verlag, New York), 3rd Ed.
2 Sridhara SG, Bai S, Shigiltchoff O, Devaty RP, Choyke WJ (2000) Differential absorption measurement of valence-band splittings in 4H SiC. *Mater Sci Forum* 338–342:567–570.
3 Wei S-H, Zunger A (1996) Valence band splittings and band offsets of AlN, GaN, and InN. *Appl Phys Lett* 69:2719–2721.
4 Lawaetz P (1971) Valence-band parameters in cubic semiconductors. *Phys Rev B* 4:3460–3467.